Azimuthal Angle Correlations for Higgs Boson plus Multi-Jet Events

Jeppe R. Andersen[a], Ken Arnold[b], Dieter Zeppenfeld[b]

[a]Theory Division, Physics Department, CERN, CH-1211 Geneva 23, Switzerland
[b]Institute for Theoretical Physics, Karlsruhe Institute of Technology, D-76128 Karlsruhe

January 21, 2010

Abstract

At lowest order in perturbation theory, the scattering matrix element for Higgs boson production in association with dijets displays a strong correlation in the azimuthal angle between the dijets, induced by the CP-properties of the Higgs Boson coupling. However, the phase space cuts necessary for a clean extraction of the CP-properties simultaneously induce large corrections from emissions of hard radiation and thus formation of extra jets. The current study concerns the generalization of CP-studies using the azimuthal angle between dijets beyond tree-level and to events with more than just two jets. By analyzing the High Energy Limit of hard scattering matrix elements we arrive at a set of cuts optimized to enhance the correlation, while maintaining a large cross section, and an observable, which is very stable against higher order corrections. We contrast the description of Higgs boson production in association with jets at different levels: for tree-level hjj and $hjjj$ matrix elements, for hjj matrix elements plus parton shower, and in a recent all-order framework, which converges to the full, all-order perturbative result in the limit of large invariant mass between all produced particles.

1 Introduction

One of the prime goals of experiments at the CERN Large Hadron Collider (LHC) is the search for the Higgs boson(s) which, within the Standard Model (SM) and many of its extensions, provide direct access to the dynamics of electroweak symmetry breaking. Once discovered, the focus of Higgs physics will turn to the study of Higgs boson properties, like its mass, spin, CP parity and the strength and structure of Higgs boson couplings to heavy fermions and gauge bosons.

Among the various Higgs channels at the LHC, the production of a Higgs boson in association with two energetic jets has emerged as particularly promising in providing information on the dynamics of the Higgs sector. For a SM-like Higgs boson, the vector boson fusion process, $qq \to qqh$, is expected to provide Higgs signals in the $h \to W^+W^-$ [1], $h \to \tau^+\tau^-$ [2,3], and/or $h \to \gamma\gamma$ [4] decay channels [5,6], depending on the Higgs boson mass, and produce crucial information for extracting the size of Higgs boson couplings [7–9]. A second important source of Higgs plus 2-jet events are gluon fusion processes, such as $qq \to qqh$, $gq \to gqh$ or $gg \to ggh$ [10]. For favorable values of the Higgs boson mass, gluon fusion induced hjj events should be visible at the LHC in the $h \to W^+W^-$ [11] and $h \to \tau^+\tau^-$ [12,13] channels.

Even in the presence of substantial SM backgrounds, the azimuthal angle correlations of gluon fusion induced hjj events can be used for establishing CP properties of the interactions of the Higgs boson [11–13]. In a SM-like situation, the Higgs interaction with gluons is mostly

mediated by a top-quark loop. For a Higgs boson which is lighter than the top quark, the resulting hjj cross section can be determined to good approximation by an effective Lagrangian of energy dimension five, which is given by [10, 14]

$$\mathcal{L}_{\text{eff}} = \frac{y_t}{y_t^{SM}} \cdot \frac{\alpha_s}{12\pi v} \cdot h\, G_{\mu\nu}^a\, G^{a\,\mu\nu} + \frac{\tilde{y}_t}{y_t^{SM}} \cdot \frac{\alpha_s}{8\pi v} \cdot A\, G_{\mu\nu}^a\, \tilde{G}^{a\,\mu\nu} \,, \tag{1}$$

where $G_{\mu\nu}^a$ denotes the gluon field strength and $\tilde{G}^{a\,\mu\nu} = 1/2\, G_{\rho\sigma}^a\, \varepsilon^{\mu\nu\rho\sigma}$ its dual. $y_t^{SM} = m_t/v$ is the SM Yukawa coupling of the Higgs boson to top quarks. The two terms result from a $\bar{t}th$ and a $\bar{t}i\gamma_5 tA$ coupling of the (pseudo)scalar Higgs, respectively, and they lead to distinctively different distributions of the azimuthal angle between the two jets: the CP-even hgg coupling produces a minimum for $\phi_{jj} = \pm\pi/2$ while a CP-odd Agg coupling leads to minima at $\phi_{jj} = 0$ and $\pm\pi$. The azimuthal angle modulations get particularly pronounced when the two jets are widely separated in rapidity. Equivalent effects are expected in vector boson fusion and have been discussed in [15, 16] for the idealized situation of parton level events at leading order (LO).

For a more realistic simulation of hjj events, effects from multiple parton emission must be included, i.e. a full parton shower analysis with subsequent hadronization and jet reconstruction should be performed. There are two effects which may substantially reduce the azimuthal angle correlations predicted with LO matrix elements: (i) the emission of additional gluons between the widely separated jets may lead to a decorrelation of azimuthal angle distributions and (ii) even the very definition of the two tagging jets becomes ambiguous in the multi-jet environment which is expected after parton shower.

A first analysis of hjj events with full parton shower simulation was performed by Odagiri [17], which, however, was built on LO $gg \to h$ hard matrix elements which do not provide the full dynamics of non-trivial azimuthal angle correlations of the produced partons. A subsequent HERWIG analysis with parton shower corrections to hard matrix elements for LO Higgs + 2 and Higgs + 3 parton production [18] indicated that parton shower effects do lead to some deterioration of the azimuthal angle correlations of the two leading jets (defined as the highest transverse momentum jets). The observed deterioration was larger, however, than what was observed in a full NLO calculation of hjj production in the effective Lagrangian approximation [19]. This discrepancy suggests that a parton shower approach generically leads to an underestimate of jet azimuthal angle correlations. The most likely cause is that the parton shower generates radiation which is basically flat in azimuthal angle and, hence, all events, where one of the tagging jets arises purely from the parton shower, have lost the azimuthal correlation. In addition, hard radiation can lead to substantial changes in the angle of the selected tagging jet which results in further decorrelation.

The full complexity of the jets in terms of the particles arising from the shower initiated by a few hard partons can only be described within a general purpose Monte Carlo [20–22] with a hadronization model. However, the description reached in such models by starting from soft- and collinear approximations may not be satisfactory for the *hard* (in transverse momentum), *perturbative* corrections; the description of the hard radiation can be repaired by matching [23–25] to fixed order calculations; but this means that the effects of such hard emissions are not resummed, and furthermore, virtual corrections (and the resulting weighting of samples with varying jet multiplicity) are estimated using only the Sudakov factor from the shower. When the interest is in the number of jets and their topology, rather than the description of the constituents of each jet, then the hard, multi-parton matrix elements can be approximated to all orders, based on the factorization properties of the scattering matrix element in the limit of large invariant mass between each hard particle, known as the *High Energy Limit* or *Multi-Regge-Kinematics* [26–28]. These ideas were developed further in Ref. [29–32], where a partonic

Monte Carlo program was constructed, which captures to all orders the leading logarithmic behavior for emissions under large invariant mass.

The goal of the present paper is two-fold. First, we present an improved observable, replacing the azimuthal angle between the leading jets as a probe for the CP-properties of the Higgs coupling to heavy quarks. The improvements are then assessed by simulating Higgs events in association with two or more jets at different levels of complexity. In Section 2 we first discuss how insight into the structure of the perturbative corrections in the High Energy or *Multi-Regge Kinematic* (MRK) limit can assist in designing observables, which extract the relevant kinematic information of the Higgs Boson vertex and are stable against higher order corrections. The resulting redefinition of the azimuthal angle between the two final state partons, in terms of the angle between jet clusters, is then first probed in Section 3, where we compare results for full fixed order matrix elements: the tree-level calculations for hjj and $hjjj$ production are juxtaposed and the idealized final states in the two- and three-parton configurations are used for deriving upper bounds on the azimuthal angle correlations which can be expected in a full simulation. For this full simulation we compare two approaches in Section 4: the conventional parton shower is generated with HERWIG++ [20] while the *Multi-Regge Kinematics* is simulated with the programs developed in Refs. [29–32]. A summary and final conclusions are drawn in Section 5.

2 Lessons From the High Energy Limit

In this section we will discuss how the insight into the structure of the perturbative corrections in the MRK limit can assist in designing observables, which extract the relevant kinematic information of the Higgs Boson vertex and are stable against higher order corrections.

The MRK limit of the $2 \to n$ scattering process is characterized by a large invariant mass between each of the produced particles, each of a fixed, perturbative transverse momentum. Specifically, for the scattering resulting in jets with momenta $p_1, \cdots, p_n$, the MRK limit is given by

$$
\begin{aligned}
&\forall i \in \{2, \ldots, n-1\} : y_{i-1} \gg y_i \gg y_{i+1} \\
&\forall i,j : |\mathbf{p}_{i\perp}| \approx |\mathbf{p}_{j\perp}|, \quad |\mathbf{q}_{i\perp}| \approx |\mathbf{q}_{j\perp}|.
\end{aligned}
\tag{2}
$$

Here $\mathbf{q}_{i\perp}$ is the transverse part of the momentum of the ith t-channel propagator, defined as $q_i = p_a - \sum_{j=1}^{i} p_j$.

In this extreme kinematic limit, the hard scattering matrix element simplifies for two reasons:

1. The contribution to jet production is dominated by the partonic channels which allow a color octet exchange between all pairs of neighboring particles in rapidity. Furthermore, in the MRK limit all such partonic channels have a universal behavior, dictated by the residues in t-channel momenta (see Ref. [31, 32] for more details).

2. The kinematic invariants relevant for the description of the dominant part of the scattering amplitude simplify in the MRK limit, resulting in a dependence on transverse momenta only.

Recent efforts [29–32] have concentrated on developing a formalism exploiting the universality of the dominance of t-channel poles (point 1), without introducing unnecessary kinematic approximations, thus obtaining a formalism which can be applied with good results away from the strict MRK limit. However, the discussion in the remainder of this section will be based on applying the full kinematic approximations of this limit.

In the MRK limit, the square of the tree-level hard scattering matrix element takes the following form for Higgs boson production in association with n gluon jets, when the rapidity of the Higgs boson is in-between jets j and $j + 1$:-

$$|\mathcal{M}_{gg \to g \cdots ghg \cdots g}|^2 \to \frac{4\hat{s}^2}{N_C^2 - 1} \left(\prod_{i=1}^{j} \frac{C_A \ g_s^2}{\mathbf{p}_{i\perp}^2} \right) \frac{|C^H(\mathbf{q}_{a\perp}, \mathbf{q}_{b\perp})|^2}{\mathbf{q}_{a\perp}^2 \ \mathbf{q}_{b\perp}^2} \left(\prod_{i=j+1}^{n} \frac{C_A \ g_s^2}{\mathbf{p}_{i\perp}^2} \right), \qquad (3)$$

where $\mathbf{q}_{a\perp} = -\sum_{i=1}^{j} \mathbf{p}_{i\perp}$, where j is the number of gluons with rapidity smaller than that of the Higgs boson, and $\mathbf{q}_{b\perp} = \mathbf{q}_{a\perp} - \mathbf{p}_{h\perp}$. In this limit, the contribution from quark-initiated processes is found by just a change of one color factor $C_A \to C_F$ for each incoming gluon replaced by a quark. The effective vertex for the coupling of the Higgs boson to two off-shell gluons through a top loop is in the combined large-m_t and MRK limit [33]

$$C^H(\mathbf{q}_{a\perp}, \mathbf{q}_{b\perp}) = i \ \frac{A}{2} \left(|\mathbf{p}_{h\perp}|^2 - |\mathbf{q}_{a\perp}|^2 - |\mathbf{q}_{b\perp}|^2 \right),$$
$$A = \frac{y_t}{y_t^{SM}} \ \frac{\alpha_s}{3\pi v}, \quad v = 246 \text{ GeV.} \qquad (4)$$

Since $p_h = q_a - q_b$, C^H is given by

$$C^H(\mathbf{q}_{a\perp}, \mathbf{q}_{b\perp}) = -i \ A \ |\mathbf{q}_{a\perp}| \ |\mathbf{q}_{b\perp}| \ \cos(\phi_{\mathbf{q}_{a\perp}\mathbf{q}_{b\perp}}) = -i \ A \ \mathbf{q}_{a\perp} \cdot \mathbf{q}_{b\perp} \qquad (5)$$

In the case of a CP-odd coupling of a pseudo-scalar to the fermions in the loop, the high-energy factorization properties and the formula in Eq. (3) still hold, with C^H replaced by

$$C^A(\mathbf{q}_{a\perp}, \mathbf{q}_{b\perp}) = i \ B \ |\mathbf{q}_{a\perp}| \ |\mathbf{q}_{b\perp}| \ \sin(\phi_{\mathbf{q}_{a\perp}\mathbf{q}_{b\perp}}) = i \ B \ (\mathbf{q}_{a\perp} \times \mathbf{q}_{b\perp}) \cdot \hat{z}, \qquad (6)$$

where $\hat{z}$ is a unit vector along the beam axis whose sign is given by the z component of $q_a - q_b$. In the notation of Ref. [11],

$$B = \frac{\tilde{y}_t}{y_t^{SM}} \ \cdot \ \frac{\alpha_s}{2\pi v}. \qquad (7)$$

The CP-properties of the coupling of the (pseudo-) scalar are reflected in the dependence on the azimuthal angle between q_a and q_b of the effective vertex for the coupling to gluons via a fermion loop (e.g. C^H or C^A). It is this dependence that the observables and cuts should emphasize. In the case of Higgs boson production in association with just two jets, $\mathbf{q}_{a\perp}, \mathbf{q}_{b\perp}$ are (up to a sign) given by the transverse momentum of the jets (at lowest order in perturbation theory), and thus the CP-properties of the Higgs boson coupling can be extracted by studying the azimuthal angle between the two jets [15].

Eq. (3) is valid for the rapidities of the Higgs boson within the rapidity interval spanned by the partons. In fact, the factorization of the amplitude into a part which depends on the momenta of the partons with rapidities much smaller than that of the Higgs boson, a Higgs boson vertex, and a function depending on the momenta of partons with rapidities much larger than that of the Higgs boson is valid also when no requirement is placed on the invariant mass between the partons on either side of the Higgs boson [34]. Therefore, we will divide the observable jets into two groups and require that all jets are well separated from the Higgs boson direction,

$$\exists j_a : y_{j_a} < y_h, \quad \exists j_b : y_{j_b} > y_h,$$
$$\forall j \in \{\text{jets}\} \ : \ |y_j - y_h| > y_{\text{sep}} \qquad (8)$$

In the following we always use the k_t jet algorithm as implemented in Ref. [35] with $R = 0.6$ and investigate jets with a transverse momentum greater than 40 GeV.

While it is clear that in LO hjj production the CP-structure of the Higgs boson vertex can be revealed by studying the azimuthal angle between the two jets, the question arises which angle to study in events with more than two jets. Traditionally, the observable applied to extract the CP structure has been the azimuthal angle between the hardest jets of the event [11,16,18], within a set of cuts based on the rapidity separation between the two hardest jets. However, Eqs. (3)-(5) suggest that the CP structure is more clearly revealed if instead the azimuthal angle between q_a and q_b is studied, with

$$
q_a = \sum_{j \in \{\text{jets}: y_j < y_h\}} p_j, \qquad q_b = \sum_{j \in \{\text{jets}: y_j > y_h\}} p_j,
$$
$$
\phi_2 = \angle(\mathbf{q}_{a\perp}, \mathbf{q}_{b\perp}) \tag{9}
$$

In the MRK limit, $(1/\sigma \; d\sigma/d\phi_2)$ is stable against higher order corrections, in so far as soft radiation, which is not picked up as jets, does not impact the angular distribution.

3 Fixed Order Studies

3.1 Tree level studies for hjj production

We start by studying the tree-level predictions for hjj production for a 14 TeV proton-proton collider and a Higgs boson mass of 120 GeV. We use the central pdf set from MSTW2008 [36], and initially we use a minimum set of cuts:

$$
p_{j\perp} > 40 \text{ GeV}, \quad y_{ja} < y_h < y_{jb}, \quad |y_{ja,jb}| < 4.5. \tag{10}
$$

The main conclusions of this study are insensitive to the choice of renormalization and factorization scale. In the hjj-analysis we set $\alpha_s^4 \to \alpha_s(p_{ja\perp})\alpha_s(p_{jb\perp})\alpha_s^2(m_H)$, with factorization scales for the pdfs of $\mu_{f,a} = p_{ja\perp}, \mu_{f,b} = p_{jb\perp}$. The matrix elements are extracted from MadGraph [37], where the $m_t \to \infty$ limit is used.

The distribution of the cross section wrt. azimuthal angle between the two jets is often distilled into a single number A_ϕ:

$$
A_\phi = \frac{\sigma(|\phi_{j_a j_b}| < \pi/4) - \sigma(\pi/4 < |\phi_{j_a j_b}| < 3\pi/4) + \sigma(|\phi_{j_a j_b}| > 3\pi/4)}{\sigma(|\phi_{j_a j_b}| < \pi/4) + \sigma(\pi/4 < |\phi_{j_a j_b}| < 3\pi/4) + \sigma(|\phi_{j_a j_b}| > 3\pi/4)}. \tag{11}
$$

This obviously gives $-1 \le A_\phi \le 1$, with $A_\phi = 0$ representing no azimuthal correlation between the jets. If there are no other sources of angular dependence, then a CP-even coupling of the Higgs boson to two off-shell gluons through a top-triangle leads to a positive value for A_ϕ, whereas a CP-odd coupling results in a negative value for A_ϕ.

In Fig. 1 we plot the value for A_ϕ as a function of Δy and y^* given by

$$
\Delta y = |y_{ja} - y_{jb}|, \quad y^* = y_h - \frac{y_{ja} + y_{jb}}{2}. \tag{12}
$$

The bin-size is $.25 \times .25$ units of rapidity. The insert shows the cross section per bin. Because of the requirement of the Higgs boson to be in-between the jets in rapidity, we have $0 < y^* < \Delta y/2$. We see that A_ϕ is largest when the jets are separated by a large rapidity interval (Δy large), and the Higgs boson is produced near the rapidity-center of the two jets (y^* small). This is caused by two effects:
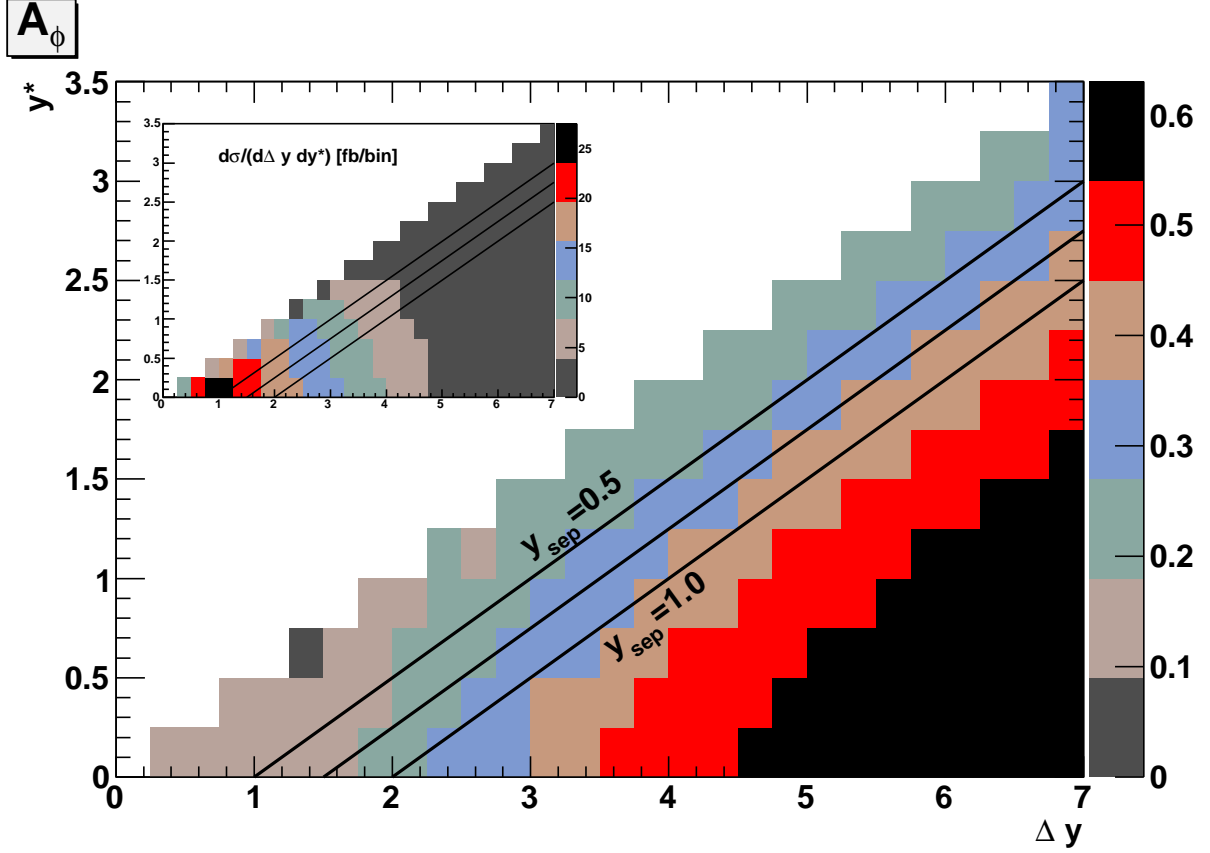
Figure 1: A_ϕ vs. Δy and y^* with a bin size of $.25 \times .25$ units of rapidity, for a SM Higgs boson of mass $m_h = 120$ GeV. Insert: $d\sigma/(dy^* d\Delta y)$ in fb/bin.

1. This kinematic setup approaches the MRK limit, where the matrix element for the gluon channels have the same kinematic dependence as the quark-initiated ones. This dependence is induced by the singularity from a gluon exchanged in the t-channel, coupling to the Higgs boson field through a top triangle. The effects of other gluon-Higgs couplings through top loops are suppressed, and only the one giving rise to the strong azimuthal correlation survives (see Ref. [29–32] for further details).

2. The azimuthal angular dependence of the t-channel propagators is suppressed, and the only azimuthal dependence left is induced by the tensor structure of $g^* g^* h$-coupling which leads to Eq. (5).

The insert in Fig. 1 shows that the cross section is peaked at $\Delta y \sim 1$ and decreases for increasing Δy and y^*. On Fig. 1 we have also indicated the limits in the $(\Delta y, y^*)$-plane corresponding to the three values $y_{\text{sep}} = 0.5, 0.75, 1$, i.e. the lines correspond to

$$\min\left(|y_h - y_{j_a}|, |y_h - y_{j_b}|\right) = y_{\text{sep}} . \tag{13}$$

Good analyzing power (large A_ϕ) and a large rate are simultaneously retained by imposing a y_{sep} cut only (as opposed to Δy and/or y^* cuts). Thus we require that the Higgs boson be produced between the jets, and that the minimum rapidity distance between the Higgs boson and the two jets be larger than a minimal value, y_{sep}.
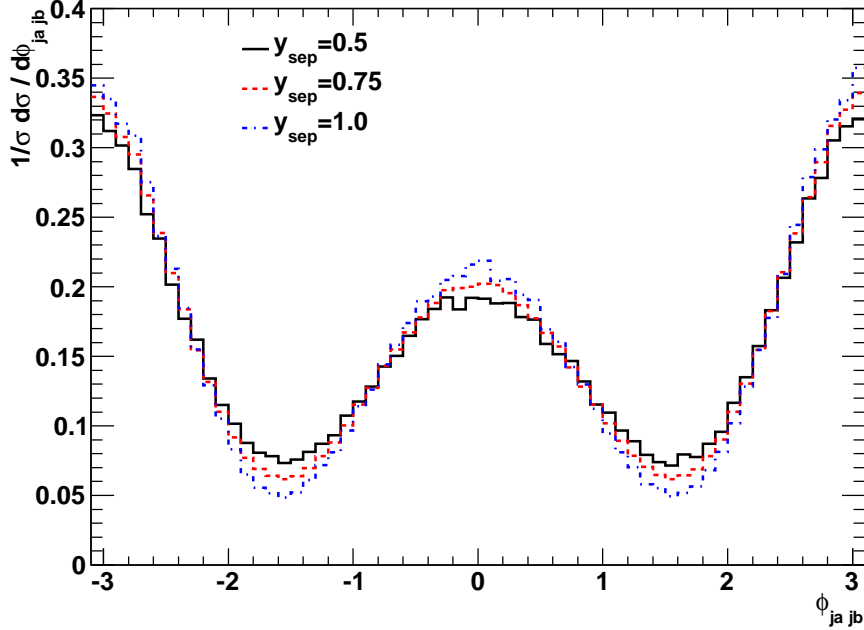
Figure 2: $(1/\sigma \; d\sigma/d\phi_{jj})$ for hjj-production at tree-level with the cuts of Eq. (14) and $y_{\text{sep}} = 0.5, 0.75, 1.0$.

Based on the findings presented in Fig. 1 and the structure of the n-jet scattering amplitude in the MRK limit given by Eq. (3), we suggest applying the following cut in Higgs boson+multi-jet samples, when the emphasis is on extracting the CP-structure of the Higgs boson coupling.

$$p_{j\perp} > 40\text{GeV}, \; \exists j_a, j_b \in \{\text{jets}\} : y_{ja} < y_h < y_{jb}, \; \forall j \in \{\text{jets}\} : |y_h - y_j| > y_{\text{sep}}, \; |y_j| < 4.5. \quad (14)$$

In Fig. 2 we plot $(1/\sigma d\sigma/d\phi_{jj})$, where ϕ_{jj} is the azimuthal angle between the two jets (defined with the sign according to Ref. [16]), with the cuts of Eq. (14) and for $y_{\text{sep}} = 0.5, 0.75, 1.0$. We see that as y_{sep} is increased, the increase in A_ϕ noted in Fig. 1 is reflected in the angular distribution approaching that of $\cos^2(\phi)$, as expected from Eq. (3)[1]. The cross section and values of A_ϕ for the series of cuts are summarized in For comparison we mention that with the same scale choices, but using the standard weak boson fusion (WBF) cuts, the LO contribution to hjj through gluon fusion is 230 fb with $A_\phi = 0.46$ (see e.g. Ref. [30] for further details). Table 1. So

y_{sep}	σ_{hjj}	A_ϕ
0.5	743 fb	0.36
0.75	553 fb	0.41
1.0	403 fb	0.45

Table 1: The value for the tree-level hjj-cross section with the cuts of Eq. (14) and three values of y_{sep}.

---

[1]Obviously, the $\cos^2(\phi)$-behavior of the cross section is reached only once not just the numerator is well approximated by that of Eq. (3), but also the t-channel propagator momenta have lost dependence on all but the transverse degrees of freedom. This is true in the MRK limit and assumed in Eq. (3), but the sub-asymptotic effects are incorporated in the formalism developed in Ref. [29–32]
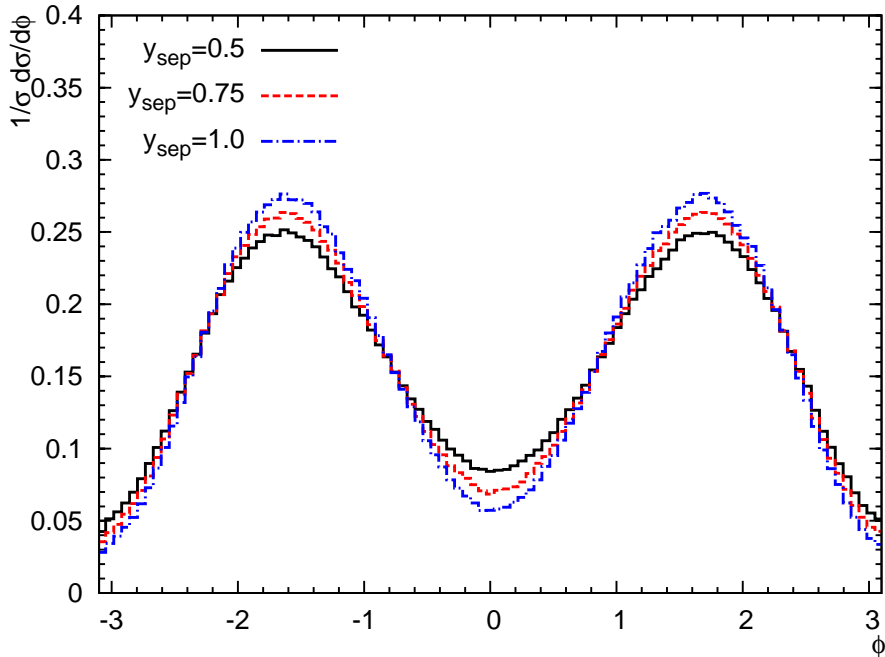
Figure 3: $(1/\sigma \; d\sigma/d\phi_{jj})$ for production of the CP-odd higgs boson A plus two jets at tree-level with the cuts of Eq. (14) and $y_{\text{sep}} = 0.5, 0.75, 1.0$. The scales were chosen as described in Section 4.1.

the cuts in Eq. (14) with $y_{\text{sep}} = 1$ display the same strong azimuthal correlation while almost doubling the cross section.

In Table 2 we list the cross sections and values of A_ϕ found for the case of a CP-odd coupling of SM-strength to a pseudo-scalar through the effective vertex of Eq. (6). We note that the magnitude of A_ϕ is almost unchanged compared to the CP-even case, just the sign is reversed. In the remainder of this study we will focus on the case of the CP-even Standard

y_{sep}	σ_{Ajj}	A_ϕ
0.5	1730 fb	-0.36
0.75	1271 fb	-0.41
1.0	908 fb	-0.46

Table 2: The value for the tree-level Ajj-cross section with the cuts of Eq. (14) and three values of y_{sep}. The scales were chosen as in Section 4.1.

Model Higgs boson. However, it is clear that the cuts and analysis developed in the following will be well suited for the extraction of the CP-parameters, even in the case of a mixture of CP-even and CP-odd couplings.

3.2 Extracting the CP-Structure with a Fit

In experimental data, there will of course be a non-negligible background to the gluon fusion hjj-signal. While the background is predominantly flat in ϕ [11–13], a flat pedestal in the distribution $(d\sigma/d\phi)$ does not leave A_ϕ invariant. We will therefore introduce a different measure

of the azimuthal correlation by fitting the distribution to the following form

$$f(\phi) \;=\; A \;+\; \frac{\pi}{2} B \; \cos(2\phi + D) \;+\; C\phi^4, \tag{15}$$

where the parameters A, B, C, D are fitted. The ϕ^4-term is found to describe well the impact of the sub-asymptotic angular dependence. In the true asymptotic form of the scattering with a CP-even coupling and no background contribution, $A = \frac{\pi}{2}B$, $D = C = 0$. For $C = D = 0$ one has $A_\phi = B/A$. A CP-odd coupling would set $D = \pi/2$. The size of B (measured in fb/rad) is a direct measure of the ability of the cuts and definition of angle in resolving the azimuthal correlation induced by the CP-nature of the Higgs boson coupling. Since in the current study we are interested in the SM Higgs couplings only, all the fits return a value for D consistent with 0. The quantity B/A measures the quality of the given sample for extracting the CP-properties. The values for B/A obtained in the fits to the hjj tree-level distributions for $y_{\text{sep}} = 0.5, 0.75, 1$ are $0.32, 0.38, 0.44$, respectively. We notice that as expected, the agreement between A_ϕ of Table 1 and B/A improves for increasing y_{sep}.

3.3 Higgs Boson Production in Association with Three Jets

We will now discuss the stability of the shape of $(1/\sigma \; d\sigma/d\phi)$ found for hjj at tree level against real emission higher order corrections within the cuts of Eq. (14), when ϕ is defined according to Eq. (9). The results of the MRK limit indicate that $(1/\sigma \; d\sigma/d\phi)$ should be stable, when ϕ is defined according to Eq. (9), rather than just the azimuthal angle between the two hardest jets. The results for the tree-level $hjjj$-cross section and the extracted A_ϕ are listed in Table 3. We note that with the definition of the azimuthal angle of the multi-jet events according to Eq. (9), for each value of y_{sep}, the extracted value for A_ϕ changes only very little compared to the values extracted from the two-jet case. For comparison, we note that if the WBF cuts are applied to the two hardest jet in the three-jet sample, the tree-level cross section for $hjjj$ is found to be just 76 fb, with $A_\phi = 0.37$ (a change of 0.09 units), when ϕ is the azimuthal angle between the two hardest jets.

The differences in the distribution $(1/\sigma \; d\sigma/d\phi)$ (with ϕ defined according to Eq. (9)) in going from the two to three-jet production is less than the differences between each neighboring curve in Fig. 2, corresponding to varying y_{sep}. The stability is a direct result of the definition of the angle according to Eq. (9), designed from the insight obtained by analyzing the MRK limit of the amplitudes, and optimized to reflect directly the CP-structure of the Higgs boson coupling. This stability in the reconstruction and extraction of the azimuthal angular dependence is encouraging for the possibility of determining the CP-properties of the Higgs boson coupling from LHC data.

In the Section 4 we will inspect the stability of this azimuthal angular dependence in two models for all-order perturbative corrections: 1) the Parton Shower model as implemented in Herwig++, supplemented with the tree-level hjj-amplitudes as described in Ref. [18], 2) a model for both the real and virtual corrections, based on the MRK limit of amplitudes, as

y_{sep}	σ_{hjjj}	A_ϕ	B/A
0.5	365 fb	0.34	0.30
0.75	232 fb	0.39	0.34
1.0	150 fb	0.42	0.41

Table 3: Values for the tree-level $hjjj$-cross section, A_ϕ and the fitted B/A ratios with the cuts of Eq. (14) and three values of y_{sep} (ϕ defined according to Eq. (9)).

discussed in Refs. [29, 30]. These studies will probe the sensitivity to the azimuthal correlation against soft radiation, which is not picked up in the visible jets, and (especially in the second case) further hard radiation. We will choose $y_{\rm sep} = 0.75$ - the specific value of $y_{\rm sep}$ does not affect the conclusions beyond the variation indicated in Tables 1-3. Larger values of the accepted cross section could be obtained by choosing a smaller value for $y_{\rm sep}$.

In the remainder of this section we will test two further predictions on the azimuthal distribution obtained from limiting behavior in Eq. (3) of the full $hjjj$-amplitude. According to the cuts of Eq. (8), the three-jet events will have two jets on one side (in rapidity) of the Higgs boson, and one jet on the other. We will call the two jets on the same side j_a, j_b, ordered according to hardness. The single jet on the other side of the Higgs boson is called j_c. First (in Section 3.3.1), we see that the distribution in the azimuthal angle defined according to Eq. (9) for three-jet events should be independent of e.g. the angle between j_a, j_b, as long as the azimuthal angle of the sum of these two jet vectors is fixed. Secondly, (in Section 3.3.2), we investigate the prediction that the strong azimuthal correlation is displayed also in events where the jets are ordered in transverse momentum as follows: $p_{\perp,j_a} > p_{\perp,j_b} > p_{\perp,j_c} > 40$ GeV, i.e. the two hardest jets are on the same side in rapidity of the Higgs boson, and the softest jet is on the other side.

3.3.1 Dependence on the Azimuthal Orientation of Two Jets

In Fig. 4 we have plotted the tree-level predictions for $(1/\sigma d\sigma/d\phi)$ for a sample of Higgs boson plus three-jet events with-in the cuts of Eq. (14) ($y_{\rm sep} = .75$), for three bins of the azimuthal angle between the two jets on one side of the Higgs boson:

$$
\begin{aligned}
S1 &: \phi_{j_a j_b} < \pi/4 \\
S2 &: \pi/4 < \phi_{j_a j_b} < 3\pi/4 \\
S3 &: 3\pi/4 < \phi_{j_a j_b} < \pi.
\end{aligned}
\tag{16}
$$

For reference, we have also plotted the distribution in the azimuthal angle in the two-jet sample. It is clear that the azimuthal dependence with the definition of Eq. (9) for the three-jet samples is extremely stable when going to the three-jet samples $S1$ and $S2$. Only for the sample $S3$ is there a slight change - this is because this sample is forced to have the two jets on one side of the Higgs boson back-to-back. Since the cross section is dominated by configurations where the jet transverse momentum is close to the lower cut-off, the sum of the transverse momenta of the two jets will typically be close to 0, and the square of the momentum of the t-channel propagator is not dominated by its transverse momentum. In other words, the last requirement of the MRK limit in Eq. (2) is violated in this sample, introducing a large dependence of the full t-channel propagator on the azimuthal orientation, so the azimuthal dependence is not described by the numerator alone. This is one reason why the formalism of Ref. [29–32] (which implements the full momentum-dependence on the t-channel propagators) offers an improvement on the BFKL formalism [26, 28, 38]. Fig. 4 also shows the fit according to Eq. (15) to each of the four distributions. It is clear that the functional form in Eq. (15) describes the distributions very well. The value for B/A obtained in the fit are $0.39, 0.35, 0.24$ for the samples $S1, S2, S3$, respectively, compared with 0.34 for the full three-jet sample with the same $y_{\rm sep} = 0.75$.

3.3.2 Dependence on the Hardness of the Three Jets

Let us now turn to the case with two harder jets on one side in rapidity of the Higgs boson, and a softer on the other side, all above 40 GeV in transverse momentum. The reason for studying these event configurations is to determine (using the full tree-level hard scattering
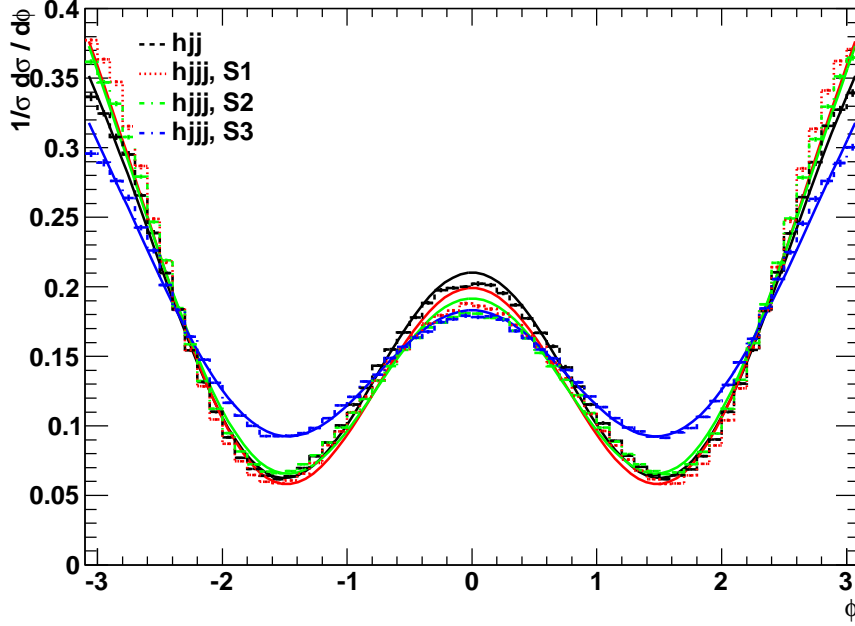
Figure 4: The angular distribution (according to Eq. (9)) for $y_{\text{sep}} = 0.75$ for both the two-jet sample and three different sub-samples of the three-jet sample (all jets above 40 GeV in transverse momentum — see text for further details). The cuts and the definition of azimuthal angle in samples of more than two jets ensure that the distribution is very stable against perturbative corrections. The lines are fits on the form of Eq. (15) to the histograms.

matrix element) whether in this skewed setup the scattering displays the angular correlation expected from the analysis in Section 2. Specifically, we choose the following cuts

$$
\begin{aligned}
& p_{\perp,j_a} > p_{\perp,j_b} > p_{\perp,j_c} > 40\,\text{GeV}, \\
& y_{j_a,j_b} < y_h < y_{j_c} \text{ or } y_{j_a,j_b} > y_h > y_{j_c} \\
& |y_h - y_j| > y_{\text{sep}}, \ |y_j| < 4.5.
\end{aligned}
\tag{17}
$$

With the standard scale-choices, the cross section passing these cuts (with $y_{\text{sep}} = 0.75$) is 82 fb, i.e. about 1/3 of the three-jet rate without the additional requirement of a special configuration of the hard jets. Note that this is exactly the fraction expected from the MRK analysis of Sec. 2: There is no preference for any of the three jets in the event to be the softest, so in 1/3 of the events in the inclusive 3-jet sample it is the jet which is separated in rapidity from the two others by the Higgs boson.

In Fig. 5 we have plotted $(1/\sigma \ d\sigma/d\phi)$ for hjj, and two different azimuthal distributions for the sample of three-jet events with these selection cuts. It is immediately clear that 1) the two hardest jets do not display even a hint of the azimuthal correlation of the two-jet sample (the only slight enhancement is when the two jets are pointing in the same azimuthal direction, with the collinear divergence regularized by the jet measure (k_t − jet, $R = 0.6$), 2) the vector sum of Eq. (9) still displays the azimuthal correlation induced by the Higgs boson vertex, with a value of B/A from the fit to Eq. (15) of 0.46. Therefore, if one is applying the observable of Eq. (9) in the analysis, then the events with the two hardest jets on one side of the Higgs boson can be included and contribute to the extraction of the Higgs boson properties. This idea is backed by the insight coming from the high energy factorization of the hard scattering matrix element.
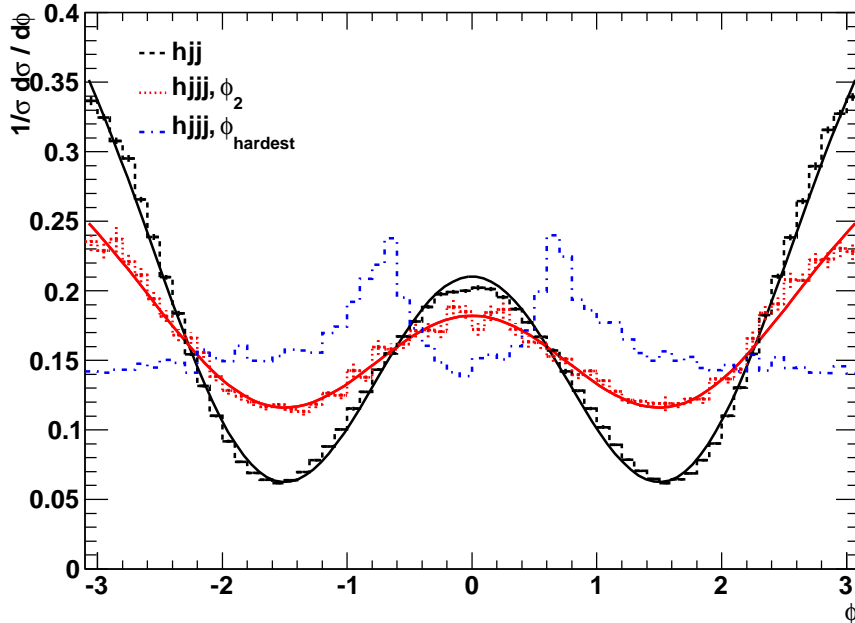
11

Figure 5: The angular distribution (according to Eq. (9)) for $y_{\text{sep}} = 0.75$ for both the two-jet sample and a three-jet (all above 40 GeV in transverse momentum) sample of the two hardest jets on one side of the Higgs and a softer on the other (see text for further details). The characteristic azimuthal dependence is not reflected in the azimuthal angle between the two hardest jets. This dependence, induced by the CP-properties of the Higgs boson couplings, is displayed however, when the sum of jet vectors according to Eq. (9) is considered. The lines are fits on the form of Eq. (15) to the histograms.

4   Correlations in a Multi-Jet Environment

4.1   Parton Shower

In order to obtain results which include higher order emissions, we used the parton level Monte Carlo VBFNLO [39] to calculate gluon fusion processes with hjj signature, generating Les Houches Event Files, which were then used as an input for the event generator HERWIG++ [20]. The renormalization scale was set to $\alpha_s^4 = \alpha_s(p_{ja\perp})\alpha_s(p_{jb\perp})\alpha_s^2(m_H)$ and the factorization scale was chosen as $\mu_f = \sqrt{p_{ja\perp} p_{jb\perp}}$. The computations were done using CTEQ6L1 parton distribution functions [40], which is different from the choice of Section 3. However, this has only minor effects and leaves the main conclusions of our findings untouched.

We generated unweighted events using the following cuts at the parton level,

$$p_{j\perp} > 30\,\text{GeV}, \qquad\qquad |y_j| < 7, \qquad\qquad |R_{jj}| > 0.3, \qquad (18)$$

and then applied the cuts of Eq. (14) on the recombined jets (which were formed using the k_t jet algorithm with a cone parameter of $R = 0.6$ as in the previous section) after the shower, hadronization and decays. An underlying event was not simulated in our studies. The choice of rather weak cuts at the matrix element level leaves the parton shower evolution a great latitude, especially concerning effects altering rapidities of the jets.

The HERWIG++ parton shower has a built in veto to forbid too hard shower emissions. The default value for the veto scale is the highest transverse momentum of the outgoing partons
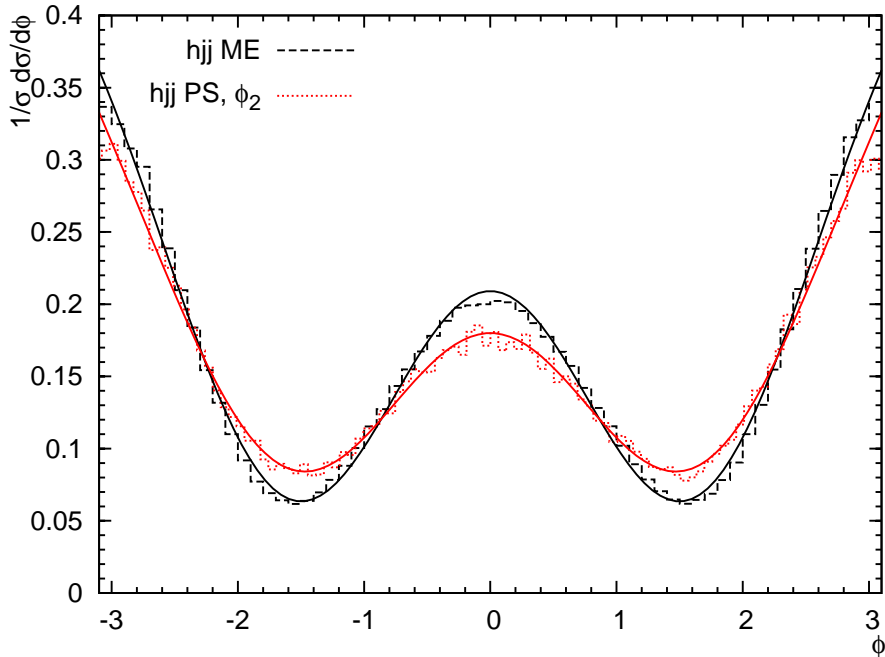
12

Figure 6: $(1/\sigma\, d\sigma/d\phi)$ for the hjj matrix element calculation and the results after parton shower, both with the cuts of Eq. (14) and $y_{sep} = 0.75$. ϕ is defined according to Eq. (9). The numbers for the azimuthal angle asymmetry measure were extracted from the fitted function.

in each event at the matrix element level. This had to be lowered to the smallest transverse momentum as, otherwise, the shower produced too many hard emissions which overcame the characteristics of the underlying process.

4.1.1 Higgs Boson Production in Association with Two Jets

Fig. 6 shows the results after the parton shower simulation for $y_{\text{sep}} = 0.75$. As expected, additional emissions created by the shower lead to a decreasing amplitude of the sinusoidal modulation, from $B/A = 0.38$ at hjj matrix element level to $B/A = 0.26$. However, the characteristics of the azimuthal angle distribution are not significantly affected by the shower. Events with exactly 2 jets of $p_T > 40$ GeV constitute 73% of the cross section. In this exclusive 2-jet sample, the shower is expected to better preserve the directions of jets which were already present in the matrix element calculation. Indeed, for this sub-sample, the fitted azimuthal asymmetry decreases by a somewhat smaller amount, to $B/A = 0.30$.

Since the contribution from events with more than 2 jets is modest, it is not surprising that the angular distribution in the 2-jet inclusive sample closely resembles the tree level result.

4.1.2 Higgs Boson Production in Association with Three Jets

The situation changes, once the parton shower is asked exclusively for events with three jets in the final state which, however, are still based on the hard hjj matrix elements. In Fig. 7, the azimuthal angle distribution for these events is plotted as the red dotted histogram and compared to the corresponding distribution at the $hjjj$ hard matrix element level (black dashed histogram), which was already shown as the red curve in Fig. 5. The difference between the results from the parton shower and that of the fixed order calculation is larger than in the exclusive 2-jet case.
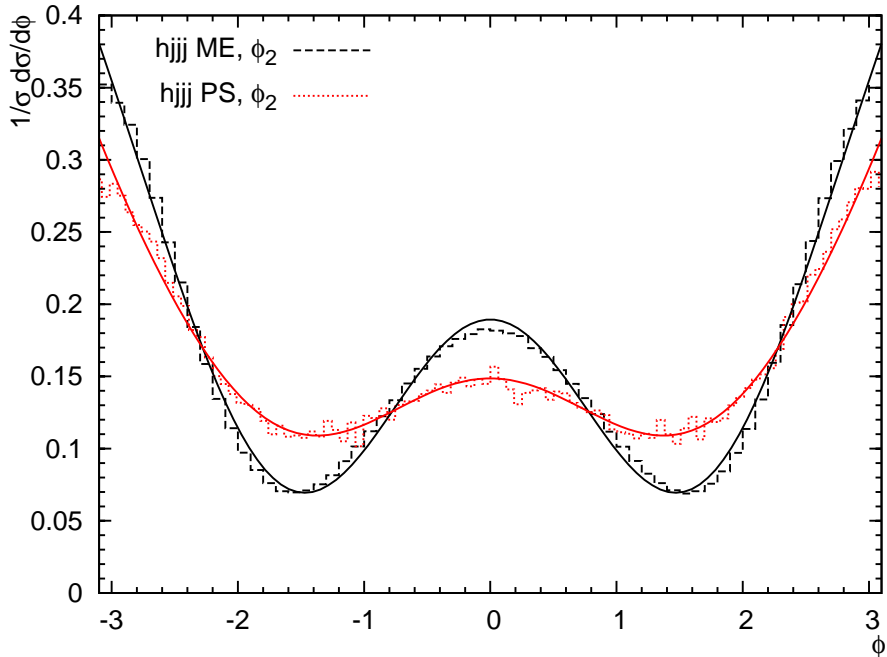
13

Figure 7: The azimuthal angle correlations for the $hjjj$ sample with transverse momentum of each jet above 40 GeV and $y_{sep} = 0.75$. The figure shows the result of the matrix element calculation and the distribution after the parton shower simulation based on the hjj matrix element calculation.

As the shower includes effects which go beyond the tree-level matrix element calculation, some additional decorrelation is expected. However, these effects of the radiation beyond that of the tree-level are small, as shown in the previous section for the exclusive two-jet sample. Rather, as we will show next, a substantial part of the decorrelation is due to phase space regions where the parton shower completely fails to produce the azimuthal angle modulation inherent in the exact matrix elements. The shower algorithm currently implemented in HERWIG++ uses only azimuthally averaged emissions, and we will in the following check the description of the three-jet events, where at least one jet must arise from the parton shower description.

Let us investigate in detail the kinematically restricted case from Section 3.3.2 with the two hardest jets j_a and j_b on one side of the Higgs Boson and the third hardest jet j_c on the other side. As noted in Section 3.3.2, this event configuration corresponds to roughly a third of the full three-jet sample in the case of the tree-level calculation. We focus on this sample, not because the parton shower emission generates a good description of the full three-jet sample, but because the failure in this particular sub-sample is so spectacular and makes it easy to draw conclusions. We demand $p_{\perp j_{a,b,c}} > 40$ GeV and the rapidity cuts of Eq. (14). The results are shown in Fig. 8(a) as the red dash-dotted histogram, while the black dashed histogram depicts the $hjjj$ fixed order calculation on parton level. Unlike the cases which were examined before, the azimuthal characteristics of the parton level appear to be completely lost and the fit returns a value of $B/A = 0.01$. The analysis was repeated with the transverse momentum of the softest jet lowered: $p_{\perp j_{a,b}} > 40$GeV, $p_{\perp j_c} > 20$GeV, in order to investigate if this hierarchy in transverse scales would help the description obtained within the parton shower. However, this did not change the azimuthal distributions noticeably, neither for the results obtained with tree-level $hjjj$ matrix elements, nor for the calculation with hjj+parton shower.
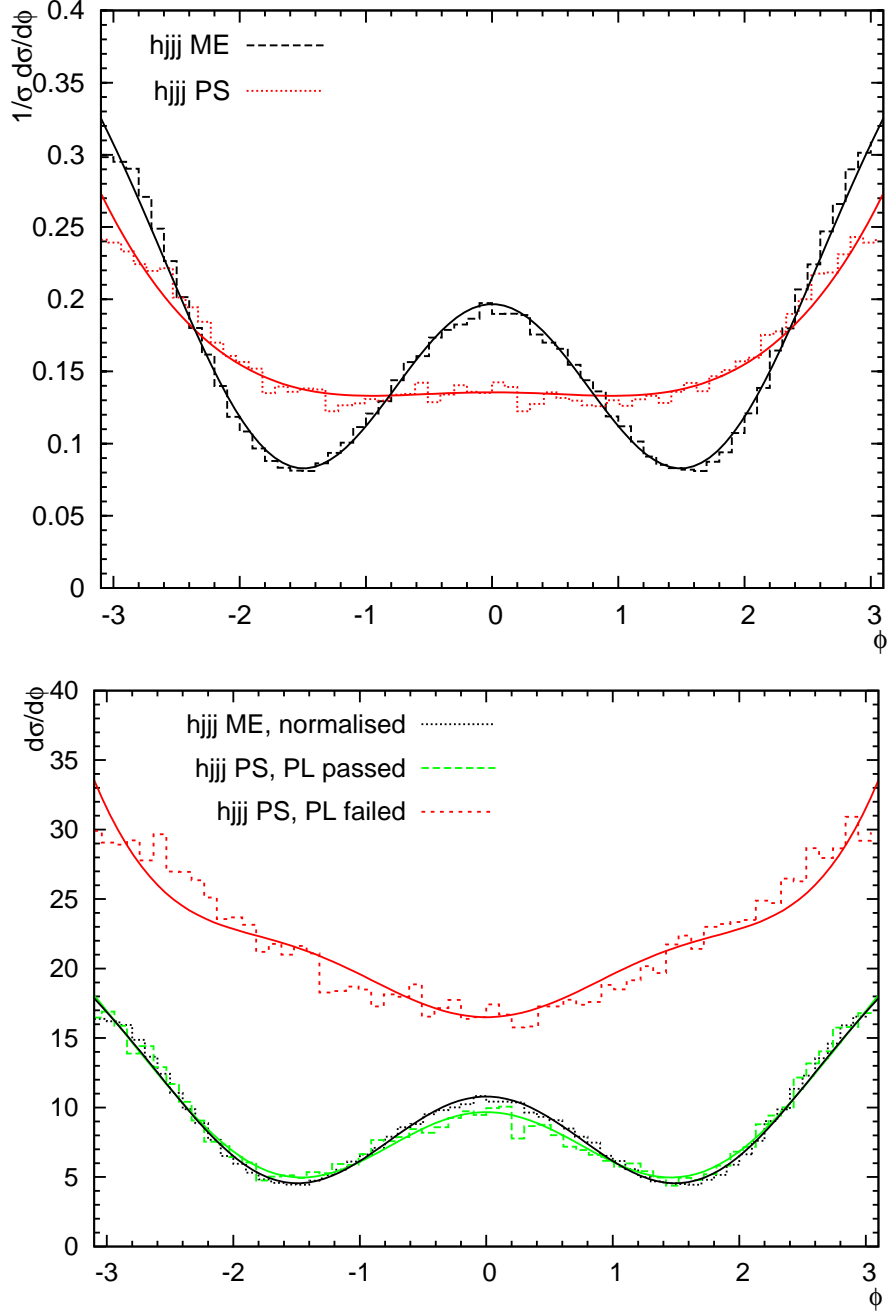
14

Figure 8: The angular distribution for $y_{sep} = 0.75$ for the sample with two hard jets on one side of the Higgs Boson and a softer (still with $p_\perp > 40\text{GeV}$) on the other. The two graphs in the upper plot depict the results of the matrix element calculation and after parton shower. The lower plot shows the observable for two different subsamples: One where the events pass the cut of Eq. (8) already on matrix element level with just two partons (denoted with 'PL passed') and one where they do not ('PL failed'). The black dotted curve is the same as in the upper plot, but normalized to the cross section of the subsample which passes the cuts at the hjj-parton level.

Figure 9: Absolute values of rapidity differences for $y_{sep} = 0.75$ for the sample with two hard jets on one side of the Higgs Boson and a softer (with $p_\perp > 40 \text{GeV}$) on the other. The blue dashed graph shows the rapidity difference between the two clusters of jets on each side of the higgs boson, after parton shower. The black dot-dashed graph shows the rapidity difference of the two partons at the matrix element level for the same sample of events. Again, this is split into two different subsamples, one where the events pass the cut of Eq. (8) at the parton level, and one where they do not.

The question why the parton shower approximation fails to describe the $hjjj$ matrix element in this special setup can be answered by having a closer look at the hard matrix element description underlying the events. One would expect the description from the parton shower to agree better with the one arrived at using the full three-jet matrix element in cases where the partonic hjj-configurations already fulfil the cuts in Eq. (14) and the two same side jets from the shower can be produced by final state collinear splittings. This is indeed the case, as shown by the green dashed histogram in Fig. 8(b). These events alone yield $B/A = 0.23$ while their complement, where the original hjj parton configurations fail the cuts of Eq. (14), have lost any azimuthal angle correlation and produce $B/A = -0.07$.

The clearest difference between events which pass at hjj parton level and those that fail can be seen by comparing rapidity separations of partons and produced clusters of jets. Fig. 9 shows the rapidity difference

$$|\Delta y| = |y_{c_a} - y_{c_b}| \tag{19}$$

of the two jet clusters c_a and c_b, which are present after the recombination of hadronic final states, as the blue dashed line. For the same sample of events, the rapidity difference of the two partons at matrix element level is plotted via the black dash-dotted histogram for all events, and this curve is split into events wich fail the cuts at parton level (red solid histogram) and those that pass (green dotted histogram). The sample with negligible azimuthal angle correlation in Fig. 8(b) was evolved from events which feature only a small rapidity separation between the

16

two outgoing partons on matrix element level and which, therefore, have both partons on the same side of the Higgs boson. The parton shower does not generate the azimuthal correlation of the clusters on opposite sides of the Higgs for such events.

As a conclusion, the question of azimuthal angle decorrelation in the setup with two hard jets on one side of the Higgs Boson and a softer one on the other is too exclusive to be handled reliably within the parton shower approximation presently implemented in HERWIG++: The azimuthal angle averaged parton shower is not the right tool for the observable in this case. It is likely, however, that the description would be improved if spin-correlations were implemented in both the parton shower [41, 42] and the interface to the matrix element.

4.2   Multi Parton Emissions from High Energy Factorization

In this section we investigate the description of the production of a Higgs boson in association with multiple jets, as described by the formalism developed in Ref. [29, 30], with the improvements of Ref. [31, 32] implemented. This results in an all-order partonic estimate of the production of a Higgs boson plus at least two jets, which is exact in the limit of large invariant mass between all (hard) partons, i.e. specifically in the limit where the real radiation produces additional hard jets. The calculation is completely exclusive in the momenta of all produced particles. We can therefore perform a detailed investigation of e.g. the jet activity in the events.

The all-order calculation results in a cross section within the cuts of Eq. (14) of 456 fb for $y_{\rm sep} = 0.75$. This is *less* than the tree-level rate (listed in Table 1). There is a reduction in the hjj tree-level cross section as a direct result of the veto of hard jets in the region of 0.75 units of rapidity either side of the Higgs boson. The exclusive jet rates found within this calculation are plotted in Fig. 10.

The exclusive hard two-jet rate amounts to just roughly 60% of the total rate within these cuts, as compared to 73% found in the study of Section 4.1 based on a parton shower of partonic hjj-states. It is therefore beneficial to ensure a solid extraction of the CP-structure of the Higgs coupling also in events with strictly more than two jets, as proposed in this study. In Fig. 11 we compare the differential distribution in the azimuthal variable defined in Eq. (9) for the tree-level hjj-calculation, and the all-order hjj-calculation of Ref. [29–32]. The stability of this distribution against higher order corrections as implemented in Ref. [29–32] is partly a result of the assumption of a dominance of the t-channel pole, but this dominance is directly verified by comparing the results of the formalism order-by-order. However, the strong correlation seen at the tree-level (as a result of the dominance of the t-channel pole) could have been spoilt in the all-order calculation by all the partons which are not included in the momenta of the hard jets, on which the azimuthal observable operates. However, as we see in Fig. 11, operating only on the momenta of the jets with a transverse momenta larger than 40 GeV still allows for a very clear extraction of the CP-structure, when the observable of Eq. (9) is used.

Finally, in Fig. 12 we compare the description of (exclusive) three-jet events between tree-level and the resummation of Ref. [29–32]. Specifically, we compare the description within the special event sample of three hard jets above 40 GeV transverse momentum, but with the two hardest on one side, and the softest at the other side (in rapidity) of the Higgs boson.

While the description of this exclusive three-jet sample differed between the description based on the full $hjjj$ matrix element and that based on hjj+parton shower, we see that the description based on Ref. [29–32] gives results which are very similar to those obtained in the calculation based on the full three-jet tree-level matrix element. This is a testament to both the quality of the all-order approximation applied, and the stability of the angular observable, defined according to Eq. (9), against higher order corrections.
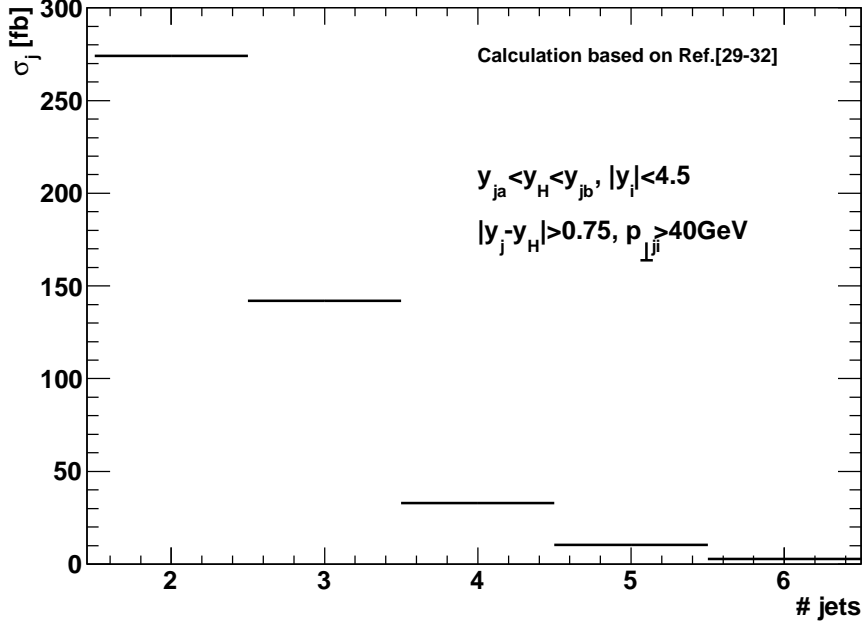
Figure 10: The exclusive jet rates within the cuts of Eq. (8) as obtained in the all-order calculation of Ref. [29–32]. All jets have a transverse momentum greater than 40 GeV.
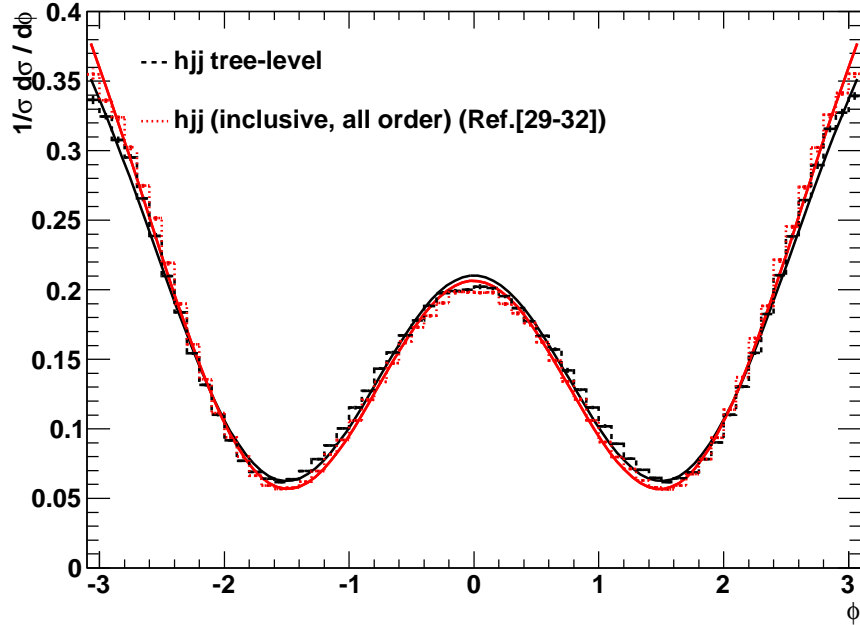

Figure 11: A comparison between the results obtained for inclusive hjj at tree-level and for the all-order approximation of Ref. [29–32] for the azimuthal correlation defined according to Eq. (9). The similarity is a testament to both the quality of the approximations in Ref. [29–32] and the stability of the observable against higher order corrections. The lines are fits on the form of Eq. (15) to the histograms.
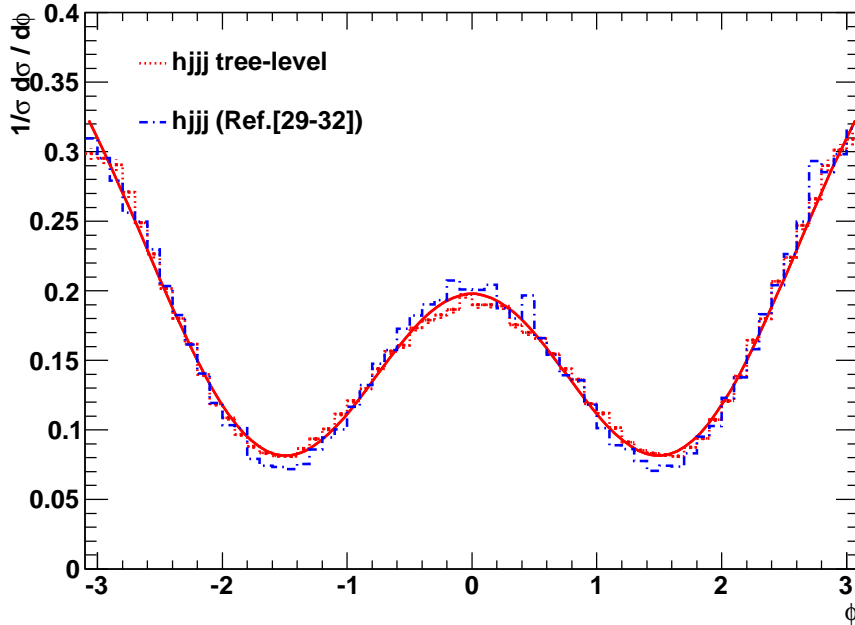
Figure 12: A comparison between the results for the azimuthal correlation defined according to Eq. (9) obtained for the exclusive $hjjj$-rate with the transverse momentum of the one jet at one side of the Higgs boson smaller than that of either jets at the other side of the Higgs boson, at tree-level and for the all-order approximation of Ref. [29–32]. The similarity is a testament to both the quality of the approximations in Ref. [29–32] and the stability of the observable against higher order corrections. The lines are fits on the form of Eq. (15) to the histograms.

5   Summary and Conclusions

Based on the analysis of the *Multi-Regge-Kinematic* (MRK) limit of the tree-level matrix elements for Higgs boson production in association with multiple jets, we optimize the extraction of the CP-properties of the Higgs boson coupling to heavy fermions in two steps. First, we have designed a set of cuts which enhances the sought-after behavior. Secondly, we generalize the azimuthal angle observable used to extract the CP-properties of the couplings in Higgs boson plus dijet events to the case of three or more jets. This is desirable, since roughly half of the inclusive Higgs-boson plus dijet sample will contain more than two jets (for a 14 TeV proton-proton collider and the cuts employed in the present analysis).

We have thoroughly tested the predictions obtained from the MRK limit against calculations using full tree-level matrix elements, and find that the expectations from the MRK limit are all respected by the full tree-level calculations, and that the constructed observable leads to an extraction of the CP-properties of the Higgs-boson couplings which is extremely stable against perturbative corrections.

We have compared the predictions for both Higgs boson plus two jet and for three-jet events obtained in two all-order perturbative approximations against the full tree-level calculation. We find that the calculation based on a parton shower evolution of the hard hjj-matrix element, while giving a good description in large areas of phase space, fails to give a satisfactory description of the three-jet states in those phase space regions, where the direct correspondence

19

of hard partons at matrix element level with the leading jets is lost. These phase space regions are numerically important. In particular, we discussed the failings in the parton-shower description of the azimuthal correlations observed in the full hard matrix element. Contrary to this, the all-order perturbative calculation based on the formalism developed in Ref. [29–32] leads to results which are in good agreement with both the exclusive two and three-parton samples checked in this study, while giving an estimate of the sensitivity of the observables to corrections beyond tree-level. Again, the observable constructed in Sec. 2 is shown to lead to an extraction of the CP-properties of the Higgs boson coupling which is extremely stable against higher order corrections.

Based on the analysis of hjj and $hjjj$ at fixed order, and the MRK-inspired all-order resummation, we conclude that, with the right choice of observable, the analyzing power of azimuthal jet correlations in hjj events for the extraction of Higgs boson CP-properties can be preserved when going from a LO analysis to a more complete and sufficiently detailed QCD description of additional parton emission. While the contribution from hard radiation beyond tree-level is significant and can jeopardize the extraction of the CP-properties, the impact of such radiation is minimized by the use of the observable advocated in Eq. (9), which depends on all the jet vectors of the event. In particular, also the NLO QCD calculation of Ref. [19] should be able to provide reliable predictions for the extraction of CP-properties in gluon fusion induced hjj events. Stronger decorrelation effects, which were observed in the past when performing parton shower simulations of hjj events [17,18] are, to a considerable extent, due to present limitations of the parton shower programs and the use of azimuthal observables, which are unstable against radiative corrections.

The current study also provides a clear demonstration of how the insight gained from the structure of scattering matrix elements in the MRK limit can assist the design of analyses at the LHC.

Acknowledgements

References

[1] D. L. Rainwater and D. Zeppenfeld, "Observing $H \to W^{(*)}W^{(*)} \to e^{\pm}\mu^{\mp}\displaystyle{\not}p_T$ in weak boson fusion with dual forward jet tagging at the CERN LHC," *Phys. Rev.* **D60** (1999) 113004, `arXiv:hep-ph/9906218`.

[2] D. L. Rainwater, D. Zeppenfeld, and K. Hagiwara, "Searching for H → tau tau in weak boson fusion at the LHC," *Phys. Rev.* **D59** (1999) 014037, `arXiv:hep-ph/9808468`.

[3] T. Plehn, D. L. Rainwater, and D. Zeppenfeld, "A method for identifying H → tau tau → e+- mu-+ missing p(T) at the CERN LHC," *Phys. Rev.* **D61** (2000) 093005, `arXiv:hep-ph/9911385`.

[4] D. L. Rainwater and D. Zeppenfeld, "Searching for H → gamma gamma in weak boson fusion at the LHC," *JHEP* **12** (1997) 005, `arXiv:hep-ph/9712271`.

[5] S. Asai *et al.*, "Prospects for the search for a standard model Higgs boson in ATLAS using vector boson fusion," *Eur. Phys. J.* **C32S2** (2004) 19–54, `arXiv:hep-ph/0402254`.

[6] **CMS** Collaboration, G. L. Bayatian *et al.*, "CMS technical design report, volume II: Physics performance," *J. Phys.* **G34** (2007) 995–1579.

[7] D. Zeppenfeld, R. Kinnunen, A. Nikitenko, and E. Richter-Was, "Measuring Higgs boson couplings at the LHC," *Phys. Rev.* **D62** (2000) 013009, `arXiv:hep-ph/0002036`.

[8] M. Duhrssen *et al.*, "Extracting Higgs boson couplings from LHC data," *Phys. Rev.* **D70** (2004) 113009, `arXiv:hep-ph/0406323`.

[9] R. Lafaye, T. Plehn, M. Rauch, D. Zerwas, and M. Duhrssen, "Measuring the Higgs Sector," *JHEP* **08** (2009) 009, `arXiv:0904.3866 [hep-ph]`.

[10] R. P. Kauffman, S. V. Desai, and D. Risal, "Production of a higgs boson plus two jets in hadronic collisions," *Phys. Rev.* **D55** (1997) 4005–4015, `hep-ph/9610541`.

[11] G. Klamke and D. Zeppenfeld, "Higgs plus two jet production via gluon fusion as a signal at the CERN LHC," *JHEP* **04** (2007) 052, `arXiv:hep-ph/0703202`.

[12] G. Klämke, *Higgs plus 2 Jet Produktion in Gluonfusion*. PhD thesis, University of Karlsruhe, 2008.

[13] G. Klämke, M. Rauch, and D. Zeppenfeld, "in preparation,".

[14] R. P. Kauffman and S. V. Desai, "Production of a higgs pseudoscalar plus two jets in hadronic collisions," *Phys. Rev.* **D59** (1999) 057504, `hep-ph/9808286`.

[15] T. Plehn, D. L. Rainwater, and D. Zeppenfeld, "Determining the structure of Higgs couplings at the LHC," *Phys. Rev. Lett.* **88** (2002) 051801, `hep-ph/0105325`.

[16] V. Hankele, G. Klamke, D. Zeppenfeld, and T. Figy, "Anomalous higgs boson couplings in vector boson fusion at the CERN LHC," *Phys. Rev.* **D74** (2006) 095001, `hep-ph/0609075`.

[17] K. Odagiri, "On azimuthal spin correlations in Higgs plus jet events at LHC," *JHEP* **03** (2003) 009, `arXiv:hep-ph/0212215`.

[18] V. Del Duca *et al.*, "Monte Carlo studies of the jet activity in higgs + 2jet events," *JHEP* **10** (2006) 016, `hep-ph/0608158`.

[19] J. M. Campbell, R. K. Ellis, and G. Zanderighi, "Next-to-leading order higgs + 2 jet production via gluon fusion," *JHEP* **10** (2006) 028, `hep-ph/0608194`.

[20] M. Bahr *et al.*, "Herwig++ Physics and Manual," *Eur. Phys. J.* **C58** (2008) 639–707, `arXiv:0803.0883 [hep-ph]`.

[21] T. Sjostrand, S. Mrenna, and P. Skands, "A Brief Introduction to PYTHIA 8.1," *Comput. Phys. Commun.* **178** (2008) 852–867, `arXiv:0710.3820 [hep-ph]`.

[22] T. Gleisberg *et al.*, "Event generation with SHERPA 1.1," *JHEP* **02** (2009) 007, `arXiv:0811.4622 [hep-ph]`.

[23] L. Lonnblad, "ARIADNE version 4: A Program for simulation of QCD cascades implementing the color dipole model," *Comput. Phys. Commun.* **71** (1992) 15–31.

[24] S. Catani, F. Krauss, R. Kuhn, and B. R. Webber, "QCD Matrix Elements + Parton Showers," *JHEP* **11** (2001) 063, `arXiv:hep-ph/0109231`.

[25] M. L. Mangano, M. Moretti, F. Piccinini, and M. Treccani, "Matching matrix elements and shower evolution for top- quark production in hadronic collisions," *JHEP* **01** (2007) 013, `arXiv:hep-ph/0611129`.

[26] V. S. Fadin, E. A. Kuraev, and L. N. Lipatov, "On the Pomeranchuk singularity in asymptotically free theories," *Phys. Lett.* **B60** (1975) 50–52.

[27] E. A. Kuraev, L. N. Lipatov, and V. S. Fadin, "Multi - Reggeon processes in the Yang-Mills theory," *Sov. Phys. JETP* **44** (1976) 443–450.

[28] E. A. Kuraev, L. N. Lipatov, and V. S. Fadin, "The Pomeranchuk singularity in nonabelian gauge theories," *Sov. Phys. JETP* **45** (1977) 199–204.

[29] J. R. Andersen and C. D. White, "A New Framework for Multijet Predictions and its application to Higgs Boson production at the LHC," *Phys. Rev.* **D78** (2008) 051501, `arXiv:0802.2858 [hep-ph]`.

[30] J. R. Andersen, V. Del Duca, and C. D. White, "Higgs Boson Production in Association with Multiple Hard Jets," *JHEP* **02** (2009) 015, `arXiv:0808.3696 [hep-ph]`.

[31] J. R. Andersen and J. M. Smillie, "Constructing All-Order Corrections to Multi-Jet Rates," *JHEP* **01** (2010) 039, `arXiv:0908.2786 [hep-ph]`.

[32] J. R. Andersen and J. M. Smillie, "The Factorisation of the t-channel Pole in Quark-Gluon Scattering," `arXiv:0910.5113 [hep-ph]`.

[33] V. Del Duca, W. Kilgore, C. Oleari, C. R. Schmidt, and D. Zeppenfeld, "Kinematical limits on Higgs boson production via gluon fusion in association with jets," *Phys. Rev.* **D67** (2003) 073003, `hep-ph/0301013`.

[34] V. Del Duca, A. Frizzo, and F. Maltoni, "Factorization of tree QCD amplitudes in the high-energy limit and in the collinear limit," *Nucl. Phys.* **B568** (2000) 211–262, `arXiv:hep-ph/9909464`.

[35] M. Cacciari and G. P. Salam, "Dispelling the n**3 myth for the k(t) jet-finder," *Phys. Lett.* **B641** (2006) 57–61, `hep-ph/0512210`.

[36] A. D. Martin, W. J. Stirling, R. S. Thorne, and G. Watt, "Parton distributions for the LHC," `arXiv:0901.0002 [hep-ph]`.

[37] J. Alwall *et al.*, "MadGraph/MadEvent v4: The new web generation," *JHEP* **09** (2007) 028, `arXiv:0706.2334 [hep-ph]`.

[38] I. I. Balitsky and L. N. Lipatov, "The Pomeranchuk singularity in quantum chromodynamics," *Sov. J. Nucl. Phys.* **28** (1978) 822–829.

[39] K. Arnold *et al.*, "VBFNLO: A parton level Monte Carlo for processes with electroweak bosons," *Comput. Phys. Commun.* **180** (2009) 1661–1670, `arXiv:0811.4559 [hep-ph]`.

[40] J. Pumplin *et al.*, "New generation of parton distributions with uncertainties from global QCD analysis," *JHEP* **07** (2002) 012, arXiv:hep-ph/0201195.

[41] I. G. Knowles, "Spin correlations in parton - parton scattering," *Nucl. Phys.* **B310** (1988) 571.

[42] J. C. Collins, "Spin correlations in Monte Carlo event generators," *Nucl. Phys.* **B304** (1988) 794.